MOLECULAR AND CELLULAR BIOLOGY, Dec. 2006, p. 9302–9314 Vol. 26, No. 24
0270-7306/06/$08.00+0 doi:10.1128/MCB.00260-06

Mammary Tumorigenesis and Metastasis Caused by Overexpression of Insulin Receptor Substrate 1 (IRS-1) or IRS-2▽

Robert K. Dearth,[1]† Xiaojiang Cui,[1]† Hyun-Jung Kim,[1] Isere Kuiatse,[1] Nicole A. Lawrence,[2] Xiaomei Zhang,[1] Jana Divisova,[1] Ora L. Britton,[1] Syed Mohsin,[1] D. Craig Allred,[1] Darryl L. Hadsell,[2] and Adrian V. Lee[1]*

Breast Center, Baylor College of Medicine and Methodist Hospital, Departments of Medicine, Molecular and Cellular Biology, and Pathology, Houston, Texas 77030,[1] and USDA/ARS Children's Nutrition Research Center, Departments of Pediatrics and Molecular and Cellular Biology, Baylor College of Medicine, Houston, Texas[2]

Received 11 February 2006/Returned for modification 10 April 2006/Accepted 18 September 2006

Insulin receptor substrates (IRSs) are signaling adaptors that play a major role in the metabolic and mitogenic actions of insulin and insulin-like growth factors. Reports have recently noted increased levels, or activity, of IRSs in many human cancers, and some have linked this to poor patient prognosis. We found that overexpressed IRS-1 was constitutively phosphorylated in vitro and in vivo and that transgenic mice overexpressing IRS-1 or IRS-2 in the mammary gland showed progressive mammary hyperplasia, tumorigenesis, and metastasis. Tumors showed extensive squamous differentiation, a phenotype commonly seen with activation of the canonical β-catenin signaling pathway. Consistent with this, IRSs were found to bind β-catenin in vitro and in vivo. IRS-induced tumorigenesis is unique, given that the IRSs are signaling adaptors with no intrinsic kinase activity, and this supports a growing literature indicating a role for IRSs in cancer. This study defines IRSs as oncogene proteins in vivo and provides new models to develop inhibitors against IRSs for anticancer therapy.

Insulin receptor substrates (IRSs) are a family of intracellular proteins that integrate and coordinate hormone, cytokine, and growth factor signaling. To date, four IRS proteins (IRS-1 to IRS-4) have been identified (27). All IRSs contain multiple tyrosine phosphorylation sites that act as binding sites for SH2-containing proteins (27). The IRS proteins were first identified as substrates and presumed signaling intermediates of the insulin receptor. However, it is now clear that the IRS proteins can be activated and phosphorylated by a number of other signaling pathways, including those that are critical for mammary gland development, such as growth hormone and prolactin (2, 56).

Much research has focused on the roles of IRSs in both metabolic and mitogenic signaling; however, the last several years have seen an emergence of literature implicating IRSs in human cancer. IRS-1 is constitutively active and phosphorylated in many tumors (6). IRS-1 levels are increased in patients with pancreatic cancer (1), and both IRS-1 and IRS-2 levels are increased in patients with hepatocellular cancer (3, 36). We previously reported that high IRS-1 levels are associated with poor outcomes for patients with breast cancer (25, 41), and this is supported by further studies showing that IRS-1 is expressed in patients with primary breast cancer and metastases, and its levels correlate with poor differentiation and lymph node involvement (22). One study, however, found that IRS-1 levels in advanced primary breast cancers were reduced compared to breasts from healthy patients (44).

The mouse mammary gland has served as a useful area for the identification and characterization of oncogenes and tumor suppressor genes important in human breast cancer (15). For example, transgenic mice overexpressing the HER-2 oncogene develop mammary cancer with biological and phenotypic variances similar to those observed in human breast cancer patients (23).

To date, there have been no reports on the transforming abilities of IRSs in vivo. To address this, we have examined the effects of IRS overexpression in vitro and in vivo. We found that IRS-1 was constitutively activated when overexpressed in cell lines, and this resulted in disruption of immortalized mammary epithelial cell acinus morphogenesis. Furthermore, transgenic mice that overexpressed human IRS-1 or IRS-2 in the mammary gland showed progressive mammary hyperplasia, tumorigenesis, and metastasis. Tumors showed a unique histopathology consisting of numerous differentiated cell lineages, expansion of putative progenitor cells, and extensive squamous differentiation, phenotypes commonly seen with activation of β-catenin. Consistent with this, IRS proteins were found to bind β-catenin in vitro and in vivo. This is the first study to show that IRSs are oncogene proteins in vivo, and it strengthens the growing literature suggesting that IRSs are critical signaling adaptor proteins in tumorigenesis.

MATERIALS AND METHODS

Materials. General materials and chemicals were purchased from Sigma (St. Louis, MO) unless otherwise noted. All tissue culture reagents were purchased from Life Technologies (Carlsbad, CA) unless otherwise stated.

Plasmid construction. Human IRS-1 cDNA was excised from pCMV-His-IRS-1 (48), human IRS-2 cDNA was excised from pLTR-IRS-2 (51), and both

* Corresponding author. Mailing address: One Baylor Plaza MS: 600, Room N1110, Baylor College of Medicine, Houston, TX 77030. Phone: (713) 798-1624. Fax: (713) 798-1642. E-mail: avlee@breastcenter.tmc.edu.

† These authors contributed equally to the work.

▽ Published ahead of print on 9 October 2006.

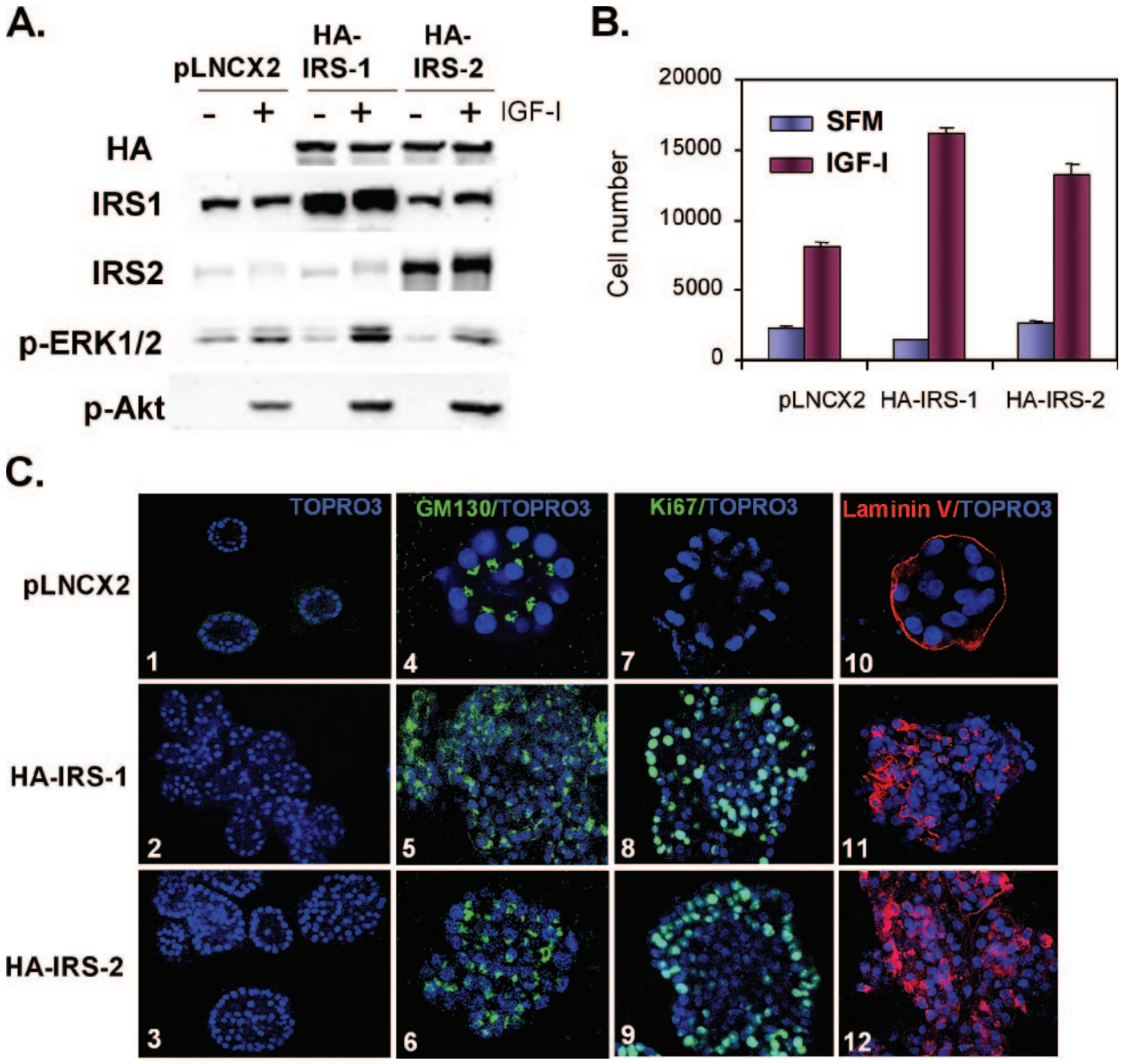

FIG. 1. Overexpression of HA-tagged IRS-1 or IRS-2 disrupts MCF-10A acinus morphogenesis. (A) Representative Western blot illustrating the generation of MCF-10A stable clones overexpressing either HA-tagged IRS-1 or IRS-2 compared to endogenous levels expressed in empty vector controls (pLXCN2). Immunoblot showing IGF-I-induced phosphorylation of ERK and Akt in both IRS-1- and IRS-2-overexpressing cell lines. (B) Bar chart depicting the growth rates (expressed in cell numbers) of MCF-10A–HA–IRS-1 and MCF-10A–HA–IRS-2 cells grown in SFM with or without IGF-I compared to that of the pLNCX2 controls. (C) Confocal images of 3D Matrigel cultures of MCF-10A-pLNCX2 (top panels), MCF-10A–HA–IRS-1 (middle panels), and MCF-10A–HA–IRS-2 (bottom panels) clones stained with nuclear stain TOPRO3 (panels 1 to 3), Ki67/TOPRO3 (panels 4 to 6), GM130/TOPRO3 (panels 7 to 9), and laminin V/TOPRO3 (panels 10 to 12).

were subcloned into pSK. Human IRS-1 and human IRS-2 in pSK were tagged on the C terminus with a hemagglutinin (HA) epitope (YPYDVPDYAS) by PCR. For IRS-1, we PCR amplified a 0.8-kb C-terminal fragment and added the HA tag by using forward (5′ GCTGCTAGCATTTGCAGGCCTAC-3′) and reverse (5′-TTAAGCTTCTAGCTGGCGTAGTCGGGGACGTCGTAGGGG TACTGACGGTCCTCTGGCTGCT-3′) primers. The same 0.8-kb fragment in IRS-1 was then replaced with the HA-tagged PCR product by restriction digestion. For IRS-2, we PCR amplified a 0.7-kb C-terminal fragment and added the HA tag by using forward (5′-TTGACGTCGGGCGTGAAGAGGCT-3′) and reverse (5′-TTAAGCTTCTAGCTGGCGTAGTCGGGGACGTCGTAGGGG TACTCTTTCACGATGGTGGCCTCC-3′) primers. The HA-tagged IRS-1 and IRS-2 were sequence verified in both directions and did not contain any alterations compared to the wild-type sequence. For eukaryotic expression, HA–IRS-1 and HA–IRS-2 were subcloned into pcDNA3.1(−). To target the expression of the human IRS transgenes to the mammary gland, we placed HA-tagged human IRS-1 or human IRS-2 under the control of the mouse mammary tumor virus (MMTV) promoter (Fig. 1A). The MMTV transgenic construct has been described previously (31). For generation of retroviral plasmids, HA–IRS-1 and HA–IRS-2 were subcloned into pLNCX2.

Cell culture, retrovirus production, and establishment of stable cell lines. The immortalized human mammary epithelial cell line MCF10A was cultured as described previously (11). Retrovirus was generated by transfection of pLNCX2-HA-IRS-1, pLNCX2-IRS-2, or pLNCX2 plasmid into PT67 packaging cells (BD PharMingen, San Diego, CA) by using Lipofectamine reagent (Life Technologies). Supernatant was harvested 48 h after transfection, and MCF10A cells were plated on 60-mm dishes the day before infection and were infected for 48 h with

1 ml of the supernatant containing retrovirus encoding HA–IRS-1 and HA–IRS-2 and empty vector (pLNCX2) as a control. Infected cells were selected with 100 μg/ml neomycin (Sigma) 48 h after infection, and individual clones were isolated 10 days later. The overexpression of the IRSs was confirmed by HA immunoblot analysis, and multiple individual positive clones were pooled together to rule out clonal artifacts. These clones were named MCF-10A–HA–IRS-1 and MCF-10A–HA–IRS-2. For the control clones, isolated individual clones ($n = 5$) were pooled together (vector–MCF-10A).

Monolayer growth assay. For growth curve experiments, cells were plated in 12-well plates at a concentration of 25,000 cells/well and the day after cells were plated was designated day 0. For the measurement of cell numbers under serum-free conditions, cells were changed with serum-free medium (SFM) at day 0. Cell numbers were counted every 2 days by using a Coulter Z Series Counter (Beckman).

Cell stimulation and proliferation assay. Cells were plated into 6-cm petri dishes at 0.5×10^6 cells per plate in growth medium and were grown for 24 h. Cells were subsequently starved in SFM for 24 h and afterwards stimulated with either vehicle or insulin-like growth factor I (IGF-I; 100 ng/ml; GroPep, Adelaide, Australia) for 15 min. Cell proliferation was performed by plating cells at 2×10^4 cells per well in 24-well plates, and triplicate wells were counted daily using a Coulter Counter.

3D Matrigel culture. MCF-10A cells were grown in Matrigel as acini as described previously (11). For nuclear staining, the acinar structures were fixed in 2% paraformaldehyde at room temperature for 20 min. Fixed structures were washed three times in phosphate-buffered saline (PBS) for 10 min each. Nuclear staining was performed by incubation for 15 min with PBS containing 5 μM TOPRO-3 (Molecular Probes) before structures were mounted with the antifade agent VECTASHIELD (Vector). Confocal analyses were performed with Nikon Eclipse E1000 confocal microscopy system.

Generation of MMTV–HA–IRS-1 and MMTV–HA–IRS-2 transgenic mice. All procedures were conducted in accordance with the *NIH Guide for the Care and Use of Laboratory Animals* (http://www.nap.edu/readingroom/books/labrats/) and were approved by the IACUC of Baylor College of Medicine. Mice were maintained on a 12-h light, 12-h dark schedule with ad libitum access to laboratory chow and water. To generate transgenic mice, a linearized XbaI-SalI fragment of the MMTV–HA–IRS-1 or MMTV–HA–IRS-2 transgene (devoid of vector sequences) was microinjected into fertilized one-cell FVB/N embryos. Transgene-positive pups were identified by PCR on tail DNA. The primers for MMTV–HA–IRS-1 consisted of a forward primer in IRS-1 (5′-GCTGCTAGCATTTGC AGGCCTAC-3′) and a reverse primer in the HA tag (5′-CGTAGTCGGGGA CGTCGTAG-3′) to give a PCR product of ~800 bp, and those for IRS-2 consisted of a forward primer (5′-TTGACGTCGGGCGTGAAGAGGCT-3′) and the same reverse HA primer as that for HA–IRS-1 to give a product of ~700 bp. The PCR conditions for IRS-1 transgenic mice were 39 cycles at 94°C for 20 s, 64°C for 30 s, and 72°C for 1 min. For IRS-2, the PCR conditions were 34 cycles at 94°C for 20 s, 60°C for 30 s, and 72°C for 1 min. Of the 40 pups born, PCR of genomic DNA from tail isolation revealed five HA–IRS-1 transgenic founder lines and two HA–IRS-2 transgenic founder lines. Founders were bred with wild-type FVB/N mice to generate female mice and were then screened for HA expression by immunoblotting of mammary gland lysates at 10 days of lactation. The transgenic line containing the highest expression of HA–IRS-1 and HA–IRS-2 was chosen for further study. Whole-mount preparations were performed on inguinal mammary glands as described previously (26).

Immunofluoresence. Mammary tumors frozen in OCT were sectioned (8 μm) and fixed in cold acetone for 10 min. Sections were washed in PBS and blocked with 10% normal goat serum for 1 h. Sections were then incubated in primary Sca-1 antibody (catalog no. 557403; BD PharMingen, San Diego, CA) at a 1:100 dilution (room temperature) for 1 h, washed for 5 min three times with PBS, and then incubated in goat anti-rat Texas Red at room temperature for 1 h. Sections were washed for 5 min three times with PBS and mounted with mounting medium with DAPI (4′,6′-diamidino-2-phenylindole) (catalog no. H-1200; Vector Laboratories).

Analysis of MTTF. The median times to tumor formation (MTTF) of 20 wild-type mice and 20 transgenic mice were analyzed by weekly palpation. For multiparous studies, mice were bred at 6 weeks of age and left to continually breed and nurse pups for 21 days. Pregnancies were noted, and after female mice had eight pregnancies, they were separated from males. The date when tumors were palpated was recorded. When tumors reached approximately 1,000 mm^3, mice were injected with BrdU 2 h prior to sacrifice. Tumors were harvested, and a representative part was cut for histological analysis; one was part frozen in OCT, and the rest was snap-frozen in liquid nitrogen and kept in −80°C until further analysis. In addition, we harvested all of the other mammary glands. If they did not contain mammary tumors, one gland was frozen in OCT, one was fixed in paraformaldehyde (PFA), and one was snap-frozen in liquid nitrogen. Lungs were divided in half; one-half was fixed in PFA, for detection of metastases, and one-half was frozen in liquid nitrogen.

Histological analysis. Serial sections (5 μm thick) were placed on Superfost Plus slides (Fisher Scientific, Fair Lawn, NJ), deparaffinized, and gradually hydrated, and immunohistochemistry was performed for mouse cytokeratin 6 (K6) (1:5,000; Covance, Berkeley, CA), cytokeratin 14 (K14) (1:10,000; Covance, Berkeley, CA), TROMA-I (keratin 8 [K8]) (1:100; Developmental Studies Hybridoma Bank, University of Iowa, Iowa City, IA), HA (1:100; Covance, Berkeley, CA), and α-smooth muscle actin (SMA) (1:9,000; Sigma, St. Louis, MO). K8 and SMA mouse mammary gland antibody stainings were carried out using a Vectastain ABC peroxidase immunodetection kit (rat immunoglobulin G [IgG]) and an M.O.M. immunodetection kit, respectively (both purchased from Vector Laboratories, Burlingame, CA). For the detection of lung metastases, sections were cut at intervals of 100 μm through one half of the lung and all sections were stained by hematoxylin and eosin (H&E) and then examined microscopically. We scored lungs positive for lung metastases if they contained lesions that contained more than 100 cells. All lesions were stained for HA by immunohistochemistry (IHC).

Immunoblotting and IP. Mammary glands and cells in culture were lysed in TNESV buffer as described previously (26). We used the following phospho-specific antibodies at the indicated dilutions: p-IGF-IR, 1:500 (Cell Signaling Technology, Beverly, MA); p-IRS-1, 1:1,000 (Biosource International, Inc., Camarillo, CA); p-Akt, 1:1,000 (Cell Signaling Technology, Beverly, MA); p-ERK1/2, 1:1,000 (Cell Signaling Technology, Beverly, MA); IGF-IR (Cell Signaling Technology, Beverly, MA) and IRS-1, 1:1,000 (Upstate Group, Inc., Lake Placid, NY); Akt, 1:1,000 (Cell Signaling Technology, Beverly, MA); extracellular signal-related kinase 1/2 (ERK1/2), 1:5,000 (Upstate Group, Inc., Lake Placid, NY); and β-catenin, 1:1,000 (BD Biosciences). For immunoprecipitation (IP), 750 μg of cell lysate was precleared by protein G-agarose beads (Zymed Laboratory, San Francisco, CA) and then incubated with 7.5 μg of HA or β-catenin antibodies overnight at 4°C. The beads were washed with the lysis buffer described above three times and resuspended in protein sample buffer before the immunoprecipitation protein was subjected to immunoblotting. Anti-rabbit or anti-mouse antibodies (Amersham Biosciences, Piscataway, NJ) were used as a secondary antibody. Blots were developed using the enhanced chemiluminesence procedure (Pierce Biotechnology, Inc., Rockford, IL) and images were acquired and densitometrically analyzed using an Alpha Innotech 7700 instrument.

Statistical analysis. Time to tumor formation was analyzed using the method of Kaplan and Meier (using Prism software), and survival curves were compared using the log rank test.

RESULTS

Overexpression of IRS-1 or IRS-2 enhances Akt and ERK1/2 phosphorylation and disrupts MCF-10A acinus morphogenesis. The immortalized and nontumorigenic mammary epithelial cell line MCF-10A has been used extensively to examine the effects of various oncogenes on acinus formation in 3D Matrigel culture. Oncogenes have been shown to disrupt acinus formation by deregulating proliferation, survival, and cell polarity. We next generated retroviruses encoding HA-tagged human IRS-1 and IRS-2, infected MCF-10A cells, and selected stable HA-positive clones that were subsequently pooled (Fig. 1A). IRS-encoding virus-infected cells contained the HA protein and had overexpressed levels of IRS-1 or IRS-2 in their respective cell lines compared to endogenous levels expressed in empty vector controls. Overexpression of IRS-1 or IRS-2 in MCF-10A cells had little effect upon phosphorylation of ERK1/2 or Akt of cells in SFM; however, when stimulated with IGF-I, MCF-10A–HA–IRS-overexpressing clones showed an increased ability to phosphorylate Akt (Fig. 1A). Surprisingly, overexpression of IRS-1 also enhanced IGF-I-stimulated ERK1/2 phosphorylation, but this didn't occur with IRS-2 (seen with three individual stable transfectants). IRS-overexpressing MCF-10A cells showed enhanced growth

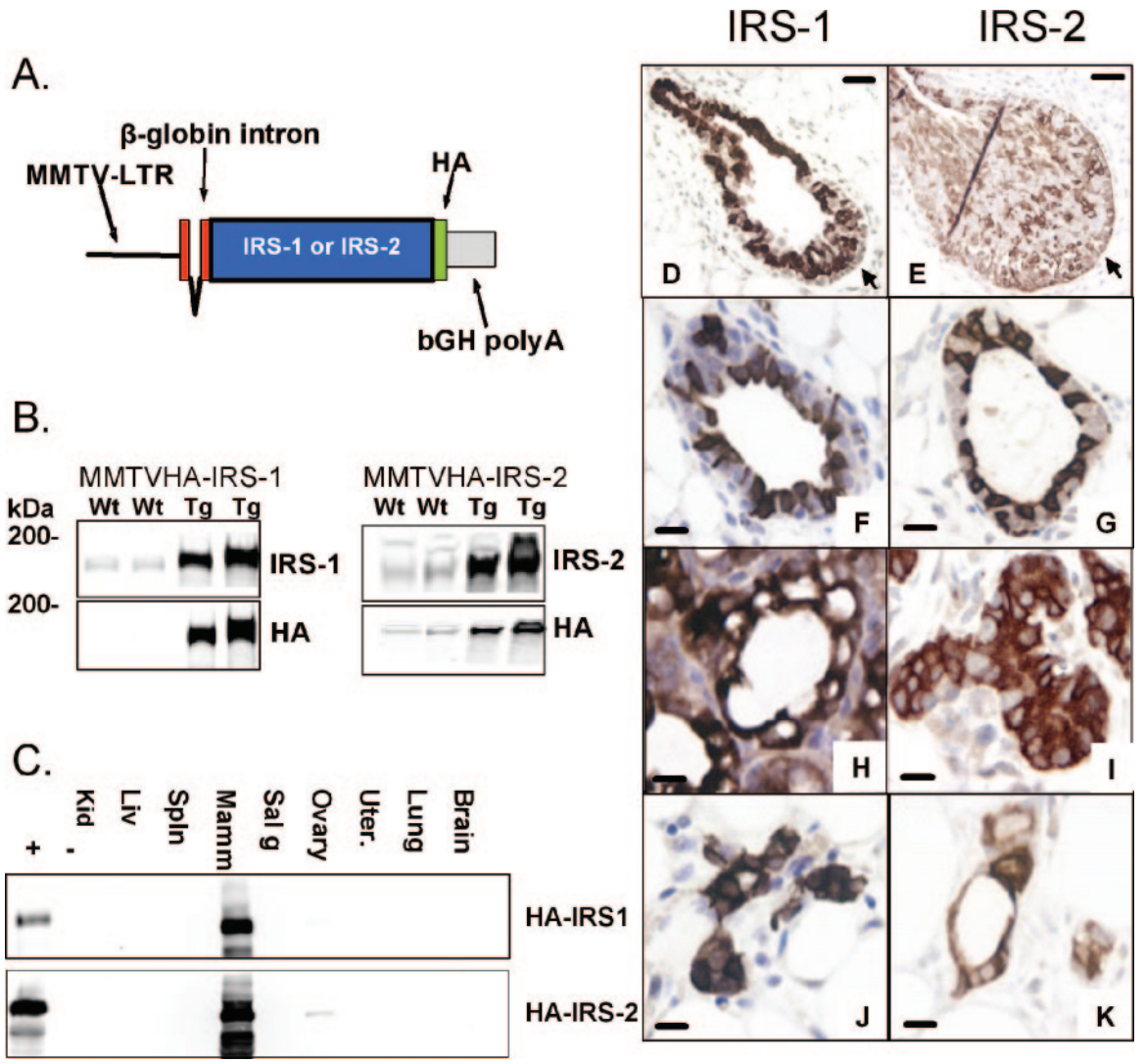

FIG. 2. Development of MMTV–HA–IRS-1 and MMTV–HA–IRS-2 transgenic mice. (A) Illustration of the MMTV-HA-IRS expression vector. bGH polyA, bovine growth hormone polyadenylation sequence. (B) Representative Western blots depicting HA, IRS-1, or IRS-2 in mammary gland lysates from transgenic (Tg) and wild-type (Wt) mice at 10 days of lactation. (C) HA immunoblotting of multiple tissue lysates from transgenic (+) and wild-type (−) mice. Kid, kidney; Liv, liver; Spln, spleen; Mamm, mammary gland; Sal g, salivary gland; Uter., uterus. (D to K) IHC staining of HA (brown cells) resulted in similar patterns of expression in mammary glands from IRS-1 (left panel) and IRS-2 (right panel) transgenic mice. Images are TEBs) (D and E) and mammary glands from 6-week-old virgin mice (F and G), mice midpregnancy (day 8) (H and I), and 4-week involuted mice (J and K). The scale bar (black) in panels D and E represents 200 μm, and that in panels F to K represents 10 μm. In panels D and E, the arrows point to the cap cell layer.

in response to IGF-I (Fig. 1B). When grown in three-dimensional Matrigel culture, MCF-10A cells underwent morphogenesis to form growth-arrested acini that stopped proliferating (absence of Ki67 staining) and were polarized with GM130 expression on the apical surface, as well as extracellular matrix component laminin V on the basal surface of the acini. Apoptosis (cleaved caspase 3 staining) was detected at day 8 when the lumen was being cleared of cells (data not shown). In stark contrast to the MCF-10A acini, MCF-10A–HA–IRS clones showed disrupted acinus formation with filling of the lumen (Fig. 1C). The overgrowth of the acini was associated with a lack of growth arrest shown by dramatic levels of proliferation (Ki67 staining), and the acini also showed a disruption of polarization with GM130 and laminin V expression present in the central cells of the lumen. Similar results have been noted with other oncogene proteins, such as Akt and HER-2 (10).

Generation and characterization of MMTV–HA–IRS-1 and MMTV–HA–IRS-2 transgenic mice. We previously established that IRS protein levels (but not mRNA levels) are dramatically influenced by developmental and hormonal signals that perpetuate normal mammary gland development (26). This, coupled with the fact that IRSs are hyperphosphorylated in breast cancer (6) and that high levels signify a poor prognosis (25), prompted us to examined the effect of IRS overexpression on mammary tumorigenesis and metastasis. We generated transgenic mice by using HA-tagged human IRS-1 or IRS-2 and utilizing the MMTV promoter (Fig. 2A). We obtained five founder mice for MMTV–HA–IRS-1 and two for MMTV–

HA–IRS-2 and examined transgene expression by immunoblotting mammary gland lysates at 10 days of lactation (Fig. 2B). HA protein was detected only in the MMTV–HA–IRS-1 and MMTV–HA–IRS-2 transgenic mice, and immunoblotting for total IRS proteins indicated that IRS-1 was overexpressed approximately 5-fold and IRS-2 was oxerexpressed 10-fold compared to endogenous levels in wild-type mice (Fig. 2B). Transgene expression was also readily detectable (albeit at a lower level than in the lactating gland) in mammary gland lysates from 6-week-old virgin mice (data not shown), and expression was highly specific for the mammary gland (Fig. 2C).

We next used IHC to determine the localization of the HA-tagged transgene expression (Fig. 2D through K). Terminal-end buds (TEBs) from both MMTV–HA–IRS-1 (Fig. 2D) and MMTV–HA–IRS-2 (Fig. 2E) transgenic 6-week-old virgin mice showed strong HA staining; however, the staining was punctate and nonuniform. HA staining was weak in the cap cell layers of MMTV–HA–IRS-1 transgenic mice, whereas it was more prominent in the cap cells of the TEBs in MMTV–HA–IRS-2 transgenic mice. As expected, we did not see any HA staining in the mammary glands of wild-type mice, confirming the specificity of this signal (data not shown). Similar to the case with TEB expression, mature ducts showed intense nonuniform staining in both MMTV–HA–IRS-1 (Fig. 2F) and MMTV–HA–IRS-2 (Fig. 2G) transgenic 6-week-old virgin mice. Mammary glands from mice midpregnancy showed intense HA staining that was then present in all epithelial cells and hence showed a more uniform pattern of staining (Fig. 2H and I). Quantitation of induction (*n*-fold) by using immunoblotting revealed an approximately fivefold induction of HA-tagged transgene expression in both MMTV–HA–IRS-1 and MMTV–HA–IRS-2 transgenic mice (data not shown). The intensity of staining increased further during lactation (data not shown). Mammary glands from mice following involution showed staining for HA in ducts from both MMTV–HA–IRS-1 and MMTV–HA–IRS-2 transgenic mice (Fig. 2J and K), but the staining was then present in all cells of the duct.

Overexpression of IRS-1 or IRS-2 causes mammary hyperplasia. We first examined the effect of HA–IRS-1 or HA–IRS-2 overexpression on normal mammary gland development and function. Analysis of ductal development from 4 to 12 weeks of age, pregnancy, and lactation indicated no obvious alterations either histologically or by whole-mount analysis (data not shown). Indeed, an analysis of lactational capacity performed by cross-fostering a fixed number of CD-1 mice and recording daily litter weight gain showed no effect of IRS overexpression during the first 10 days postpartum (data not shown).

We next examined the ability of overexpression of HA–IRS-1 or HA–IRS-2 to cause preneoplastic mammary hyperplasia. Whole-mount analysis of mammary glands from virgin mice at 24 weeks of age indicated ductal hyperplasia as a result of IRS-1 (data not shown) or IRS-2 (Fig. 3A to D) overexpression. In MMTV–HA–IRS-2 transgenic mice, these early lesions displayed a unique characteristic, in that cells appeared to bridge across ducts at regular intervals (Fig. 3A) or simply represented the filling of terminal ducts (Fig. 3B). The bridging was evident across whole sections of ducts and was found in the glands of 4/5 mice studied and was never present in the glands of wild-type mice (0/5). Sectioning and histological analysis of these bridged areas showed the presence of cells across the whole duct (Fig. 3C), which was confirmed on multiple serial sections (data not shown). The area of the duct where the cells

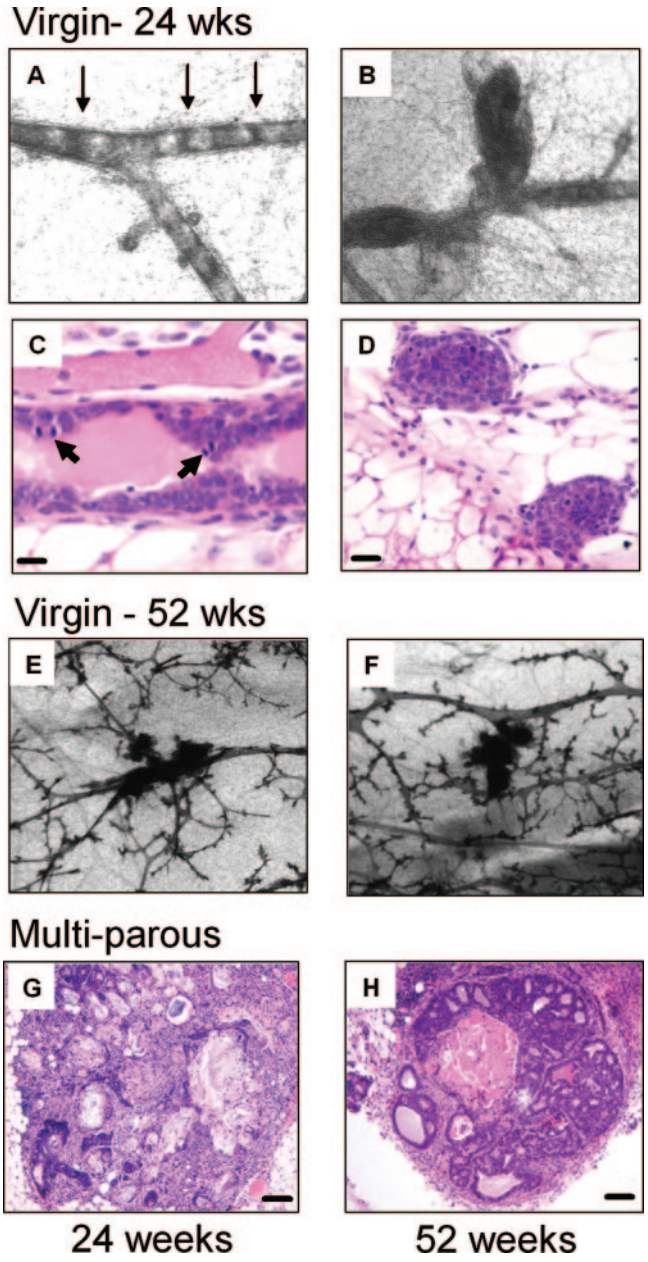

FIG. 3. Progressive mammary hyperplasia in MMTV–HA–IRS-2 transgenic mice. (A to D) Representative images showing early mammary gland hyperplasia in virgin 24-week-old MMTV–HA–IRS-2 transgenic mice. Whole-mount mammary glands (A and B) and H&E staining (C and D) illustrate the early ductal lesions and unique epithelial cell proliferation across the width of the duct (bridging of cells) highlighted by arrows (A). In panel C, arrows point to mitotic figures. The scale bar represents 10 μM. (E and F) Representative images illustrating the increase in ductal hyperplasia in virgin HA–IRS-2 transgenic mice at 52 weeks of age. H&E images of mammary gland lesions from multiparous MMTV–HA–IRS-2 transgenic mice at 24 (G) or 52 (H) weeks of age are shown. (G) Representative squamous metaplasia. (H) Representative mammary intraepithelial neoplasia.

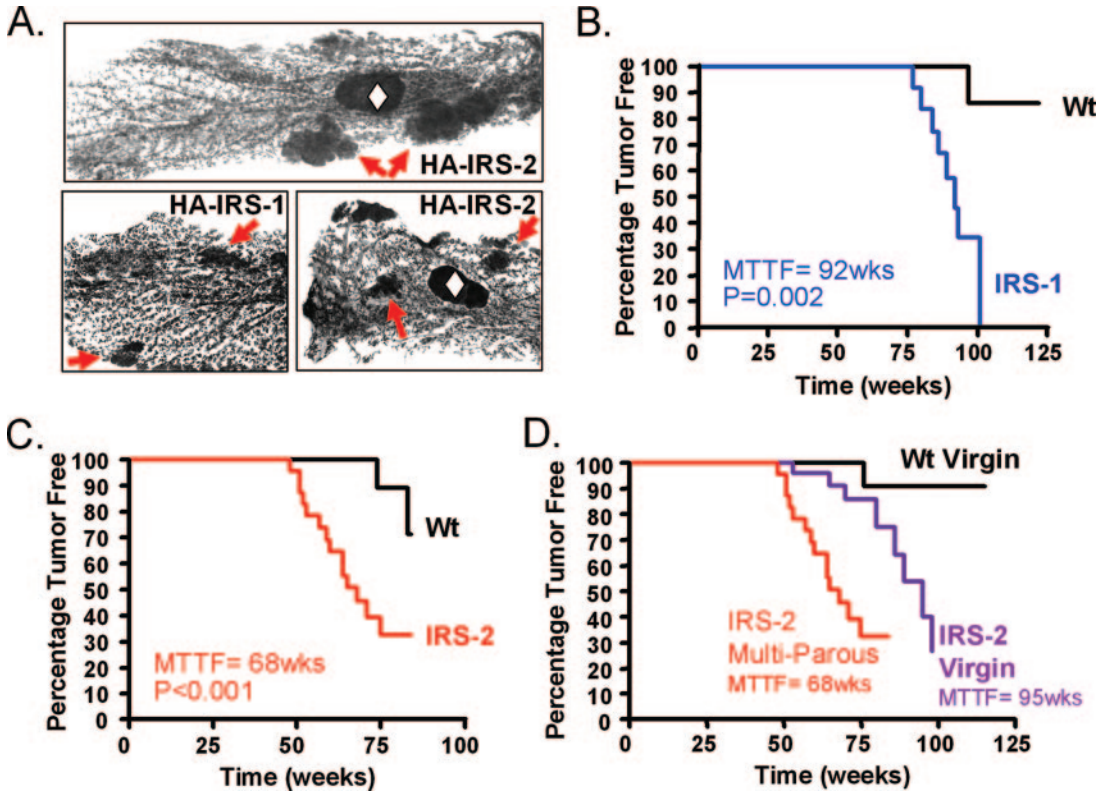

FIG. 4. Mammary tumorigenesis in MMTV–HA–IRS-1 and MMTV–HA–IRS-2 transgenic mice. Wt, wild type. (A) Whole-mount images of multiple mammary gland lesions in 18-month-old multiparous MMTV–HA–IRS-2 transgenic mice (top panel and bottom right panel) and 18-month-old MMTV–HA–IRS-1 transgenic mice (bottom left panel). Arrows point to lesions within the gland, and the open diamonds indicate the lymph nodes. (B to D) Kaplan-Meier plots illustrate the times to palpate tumors as percentages of multiparous female IRS-1 (B) or IRS-2 (C) transgenic mice compared to their respective wild-type control littermates. In addition, mammary tumor formation was significantly increased due to parity in IRS-2 transgenic mice compared to age-matched virgin controls (D). The *P* value for MTTF was calculated by the log rank test by using the Prism computer program. There were 20 mice in each group.

crossed was highly proliferative, containing multiple mitotic figures (Fig. 3C). In addition, cross sections of ducts also showed luminal filling (Fig. 3D). By 52 weeks of age, virgin mice showed an increase in the number of small lesions in the gland in both IRS-1 (data not shown)- and IRS-2 (Fig. 3E and F)-overexpressing mice. When mice were bred continuously (multiparous), we observed extensive squamous metaplasia (Fig. 3G) and lesions that resembled mammary intraepithelial neoplasia (Fig. 3H).

When mice were more than one year old, whole-mount analysis of virgin mice showed multiple tumors not only per mammary gland but in multiple glands in both IRS-1 and IRS-2 (Fig. 4A) transgenic mice. To determine the penetrance of mammary tumor formation, we used palpation to measure MTTF in multiparous (IRS-1 and IRS-2) and virgin (IRS-2) transgenic mice compared to age-matched controls. Multiparous HA–IRS-1 transgenic female mice showed palpable mammary tumors beginning at 72 weeks of age and with an MTTF of 92 weeks ($P = 0.002$) (Fig. 4B). Multiparous HA–IRS-2 transgenic female mice showed more rapid tumor formation with an MTTF of 68 weeks of age ($P < 0.001$) (Fig. 4C). Multiparous HA–IRS-2 transgenic female mice developed tumors significantly faster (MTTF, 68 weeks) than virgin mice (MTTF, 95 weeks) ($P < 0.001$) (Fig. 4D), probably due to the hormonal stimulation of MMTV transgene expression during pregnancy and lactation. We did not examine tumor formation in virgin MMTV–HA–IRS-1 transgenic mice due to the long MTTF in multiparous mice. Similar to authors of previous reports (e.g., reference 53), we did detect a few mammary tumors in aged wild-type FVB/N mice (4/60), and we found extensive pituitary hyperplasia and hyperprolactinemia (data not shown), particularly in multiparous wild-type FVB/N mice.

IRS-1 is constitutively phosphorylated in transgenic mice, and tumors show elevated levels of p-Akt and p-ERK1/2. To decipher the mechanism whereby IRSs caused tumorigenesis, we examined the effect of IRS overexpression on downstream signaling. Mammary glands from transgenic MMTV–HA–IRS-1 mice at 10 days of lactation were harvested and lysates examined for activation of HA–IRS-1. Immunoblotting of whole mammary gland lysates with a total anti-pY antibody revealed a prominent band at ~185 kDa that was present in transgenic mice but not in wild-type control littermates (Fig. 5A). Immunoblotting for total IRS-1 levels confirmed that IRS-1 levels were increased in the transgenic mice; however, the intensity of staining and migration of the total IRS-1 mirrored those of the total pY, suggesting that these are the same proteins. Immunoprecipitation with HA antibodies followed by anti-pY immunoblotting confirmed that the HA-tagged

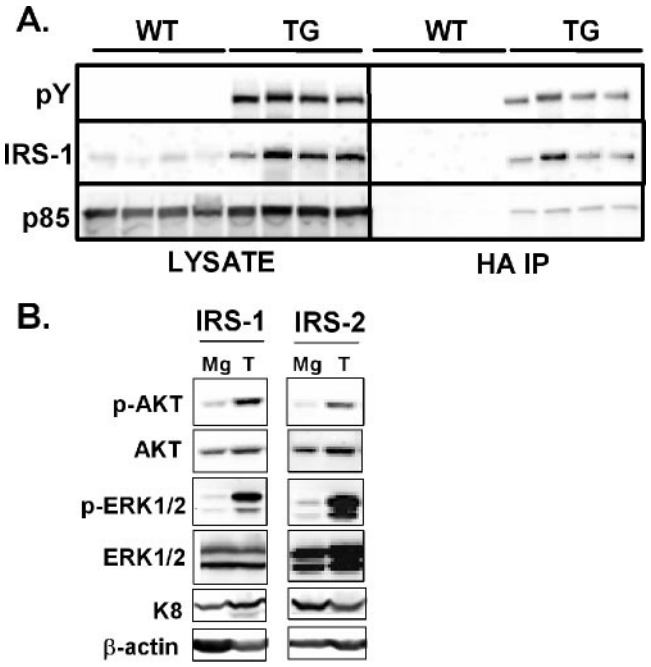

FIG. 5. Constitutive phosphorylation and p85 binding of HA–IRS-1 in transgenic mice. (A) Mammary gland lysates from MMTV–HA–IRS-1 transgenic (TG) and wild-type littermate (WT) mice at 10 days of lactation. Lysates from four independent mice (50 μg) were immunoblotted for anti-pY, total IRS-1, or p85 (left panels). Immunoprecipitation was performed on 500 μg of lysates with 5 μg of HA antibody and then probed with the same antibodies. (B) Mammary tumors (T) and mammary glands that did not contain a tumor (Mg) from the same transgenic mouse were immunoblotted for p-Akt and p-ERK1/2. Total levels were also immunoblotted as a control.

IRS-1 was constitutively phosphorylated, and this correlated with a constitutive association with the p85 subunit of phosphatidylinositol 3-kinase. IRS-1 immunoblotting upon the HA immunoprecipitation confirmed the immunoprecipitation of HA-tagged IRS-1. Despite the constitutive activation of IRS-1, we were unable to detect an increase in p-Akt or p-ERK1/2 (data not shown). We therefore examined whether the mammary gland of MMTV-HA-IRS mice would be sensitized to a bolus intravenous injection of either insulin or IGF-I. Therefore, wild-type, MMTV–HA–IRS-1, and MMTV–HA–IRS-2 mice midlactation were intravenously injected with a single bolus of either insulin (50 μg) or IGF-I (50 μg), and Akt and ERK1/2 activation levels were measured. Insulin caused a ~5-fold increase in phosphorylation levels of both ERK1/2 and Akt in wild-type mice compared the phosphylation level in mice with a saline injection. In contrast, IGF-I caused only a two- to threefold increase in phosphorylation of Akt and didn't affect ERK1/2. IGF-I or insulin activations of ERK1/2 and Akt were essentially similar in wild-type and IRS-1 and IRS-2 transgenic mice, with no apparent sensitization to either ligand.

Immunoblotting of tumors and mammary glands revealed HA expression and tyrosine phosphorylation of the HA-tagged IRSs (data not shown). ERK1/2 and Akt are well-characterized pathways downstream of IRSs and both showed increased phosphorylation in IRS-1 and IRS-2 tumors compared to mammary glands from the same transgenic mouse that didn't contain a tumor (Fig. 5B). The induction of p-ERK1/2 was seen in all IRS tumors examined, while the induction of Akt was noted in 60% of tumors.

Histology of MMTV–HA–IRS-1 and MMTV–HA–IRS-2 mammary tumors. We had predicted, based upon IRSs acting downstream of growth factor receptors, that HA–IRS-1 and HA–IRS-2 mammary tumors would consist mainly of solid adenocarcinomas similar to those seen following overexpression of other growth factor receptor signaling proteins, such as PyMT, ras, and ErbB2 (5). In stark contrast to this, both HA–IRS-1 and HA–IRS-2 mammary tumors exhibited a spectrum of histological patterns (Table 1). Examples of the types of histologies observed in MMTV–HA–IRS-2 (Fig. 6) and MMTV–HA–IRS-1 (data available upon request) are shown. Only 40% of IRS-1-induced tumors and 20% of IRS-2-induced tumors exhibited a solid nodular adenocarcinoma histology with myoepithelium or squamous metaplasia absent (Fig. 6A). Sixty percent of IRS-1 transgenic animals and 80% of IRS-2 transgenic animals had tumors exhibiting highly differentiated characteristics with ductal architecture (Fig. 6B to D and F) and/or less-differentiated tumors without ductal structure (Fig. 6E). IRS-2-induced tumors noticeably were pilar tumors that had distinguishing shaft-like neoplastic ducts consisting of keratin swirls (Fig. 6C and F) and papillary tumors, which exhibited defined cords of branched ductal architecture (Fig. 6B). The highly differentiated tumors had dense stroma with lymphocytic infiltrates (Fig. 6C and F), frequent keratinization (Fig. 6C and F), and/or glandular acinus formation with lactating properties (Fig. 6D). Extensive squamous differentiation was a characteristic histological pattern noted in the majority of the IRS tumors. Overexpression of IRS-1 did result in one specific tumor type that was not found in IRS-2 transgenic mice and was classified as a spindle cell tumor (Fig. 6E). Mammary tumors from both IRS transgenic lines were diploid, highly proliferative, and uniformly estrogen receptor and progesterone receptor negative (data not shown).

We compared the histologies of our IRS tumors with mammary tumors from transgenic mice that overexpressed a constitutively active IGF-I receptor (upstream signaling of IRS) in the mammary gland (4). We found that tumors from MMTV-CD8-IGF-IR mice also displayed dense stroma, frequent keratinization (Fig. 6G), and branched ductal architecture with glandular acinus formation, lactation (Fig. 6H), and only infrequent solid undifferentiated adenocarcinomas.

TABLE 1. Histologies of IRS mammary tumors

Tumor type	No. of tumors (% of total)	
	HA–IRS-1	HA–IRS-2
Undifferentiated (solid adenocarcinoma)	2 (40)	4 (20)
Differentiated		
Adenosquamous	1 (20)	5 (25)
Squamous cell	1 (20)	3 (15)
Spindle cell	1 (20)	0
Glandular	0	1 (5)
Papillary	0	4 (20)
Pilar	0	3 (15)

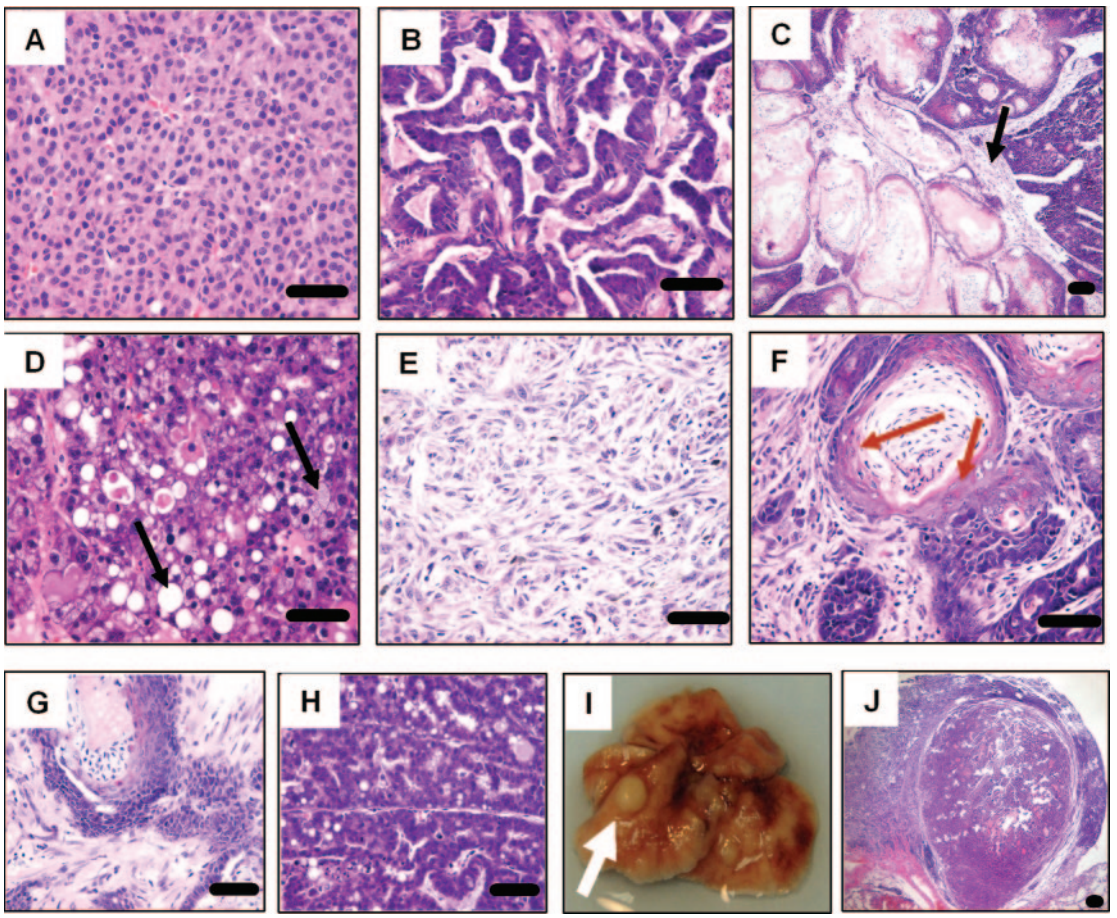

FIG. 6. Histologic characteristics of MMTV-HA-IRS mammary tumors and metastases. Representative H&E images highlighting the characteristics of IRS-1, IRS-2, or IGF-IR pathway tumors are shown. (A) IRS-2 undifferentiated solid nodular mammary tumor with sparse stroma and a lack of myoepithelial cells and squamous metaplasia. (B) IRS-2 papillary tumor with defined cords of branched ductal architecture. (C) IRS-2 pilar tumor with inflammatory infiltrates in dense, well-developed stroma (black arrow). (D) IRS-2 tumor defined by glandular acinus formation with lactation (black arrow). (E) IRS-1 spindle cell tumor. (F) Highly differentiated IRS-2 pilar tumor with dense stroma containing lymphocytic infiltrates. Red arrows show cells undergoing squamous transdifferentiation. (G) Constitutively active IGF-I receptor (CD8-IGF-IR) mammary tumor with keratinization. (H) CD8–IGF-IR mammary tumor with branched ductal architecture, glandular formation, and lactation. (I) Representative image of macroscopic lung metastases in IRS transgenic animals. (J) H&E image of lung metastasis showing characteristics of the primary mammary tumor. The scale bar (black) represents 50 μm.

MMTV–HA–IRS-1 and MMTV–HA–IRS-2 transgenic mice develop metastases. We examined the metastatic potential of MMTV-HA-IRS tumors by examining lungs from mice when tumors had reached 1,000 mm^3. Metastatic lung tumors (Fig. 6I) were observed in 33% of IRS-1 transgenic mice (1 of 3) and 40% of IRS-2 transgenic mice (10 of 25). These lung tumors presented characteristics of the primary tumor (Fig. 6J), and all stained positive for HA by IHC (data not shown). The percentage of mice showing metastases is probably an underestimate, given that we surveyed lungs only every 100 μm and we examined only half of the lung.

Expansion of putative mammary progenitor cells in MMTV-HA-IRS tumors. Overexpression of IRSs resulted in tumors with unexpected histological phenotypes. Previous studies have shown that tumor phenotype can be predicted by the transgene that is overexpressed (5). Following this theme, MMTV-HA-IRS tumors were similar to tumors generated by overexpression of activators of the canonical wnt/β-catenin signaling pathway (33, 42) which often show multiple differentiated cell lineages. As illustrated in Fig. 7A to D, highly differentiated IRS-1 tumors stained positive for the myoepithelial/myofibroblast marker α-SMA (Fig. 7A), myoepithelial cell marker K14 (Fig. 7B), and the luminal epithelial marker K8 (Fig. 7C). Likewise, highly differentiated IRS-2 tumors were positive for the same epithelial markers (data not shown). In contrast, adenocarcinomas arising in IRS-1 and IRS-2 transgenic mice were positive only for K8 and did not express K14 or α-SMA (data not shown). Highly differentiated IRS-1 (Fig. 7D) and IRS-2 (data not shown) tumors stained positive for the putative mammary progenitor cell marker K6. This staining represents an expansion of this cell population within the tumor, as wild-type mammary glands expressed very few K6-positive cells (data not shown). Additionally, differentiated IRS-2 tumors stained positive for the putative progenitor cell marker stem cell antigen-1 (SCA-1) (Fig. 7E), whereas adenocarcinomas induced by MMTV-HER-2 showed little or no SCA-1 staining (Fig. 7F). Thus, IRS tumors correlate with a class of tumors defined by expansion of putative progenitor cells and differen-

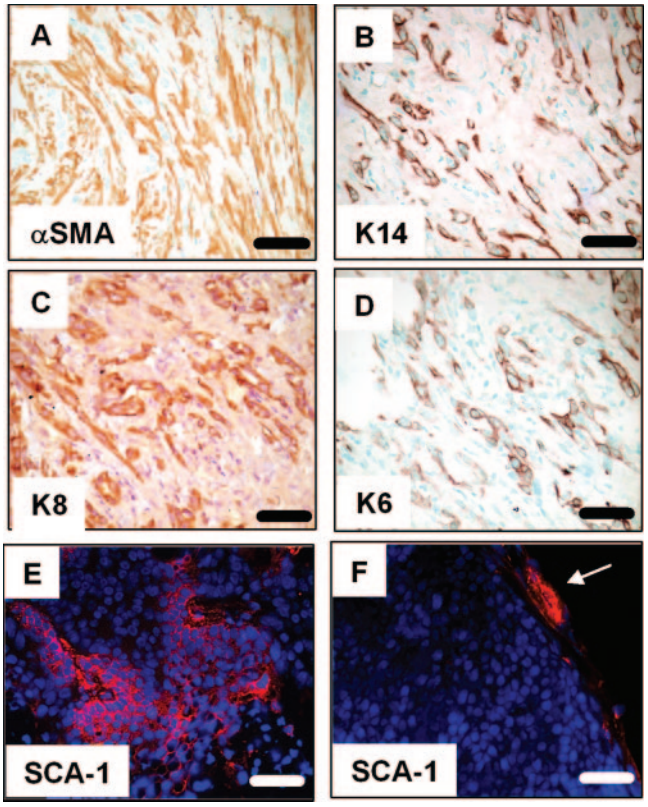

FIG. 7. MMTV-HA-IRS tumors contain luminal and myoepithelial cells and express markers of putative mammary progenitor cells. (A to C) Representative IHC for epithelial markers in a tumor from an MMTV–HA–IRS-1 transgenic mouse. (A) Anti-alpha smooth muscle actin. (B) Anti-K14. (C) Anti-K8. (D) Anti-K6 IHC on an IRS-2 tumor. (E) SCA-1 IF on an MMTV–HA–IRS-2 mammary tumor. The counterstain is DAPI (blue). (F) SCA-1 IF (red) on a mammary tumor from MMTV-HER2 transgenic mice (note the absence of SCA-1-positive staining in the tumor; positive staining is noted in the normal mammary gland periphery [white arrow]).

tiated myoepithelial and luminal epithelial cells. Importantly, we found that MMTV-CD8-IGF-IR tumors not only resembled MMTV-HA-IRS tumors in their highly differentiated phenotypes and staining for makers, such as α-SMA, K8, and K14, but also showed expansion of K6-positive cells (data not shown).

IRS proteins functionally interact with the β-catenin signaling pathway. Given the unique nature of the IRS tumors and the potential role for wnt/β-catenin in this phenotype, we examined a possible synergism between IRS and β-catenin signaling in vitro and in vivo. We therefore first examined levels of β-catenin and its downstream targets (cyclin D1 and c-*myc* genes) in IRS tumors (Fig. 8A). We observed a striking increase in β-catenin protein levels in IRS-2 (Fig. 8A) and IRS-1 (data not shown) mammary tumors. In addition, we found increased levels of the β-catenin target cyclin D1 and c-*myc* genes. Immunoblotting for K8 showed equal levels of both epithelial cell content and protein, and this was also confirmed with β-actin.

IRS-1 has recently been reported to bind and activate β-catenin (7), and so we performed coimmunoprecipitation assays to determine if this occurred in vivo and then in vitro. Reciprocal immunoprecipitation using β-catenin or HA antibodies revealed an association between the two proteins in both IRS-1 and IRS-2 tumors (Fig. 8B). We confirmed the specificity of these interactions by using control IgG (data not shown) and also by confirming the lack of interaction in cell lines that did not contain HA-IRS protein (Fig. 8C). We next investigated whether the interaction between HA-IRS and β-catenin existed in MCF-10A–HA–IRS-1 and MCF-10A–HA–IRS-2 clones. A similar association was confirmed (and absent in control MCF-10A cells), and the association of HA-IRS with β-catenin was decreased and virtually eliminated following IGF-I stimulation (for 24 h) (Fig. 8C). The interaction was confirmed by β-catenin immunoprecipitation followed by HA immunoblotting (data not shown), and specificity was also confirmed by immunoprecipitation with control IgG.

Chen et al. reported an IGF-I-stimulated association between IRS-1 and β-catenin which was associated with translocation of IRS-1 to the nucleus (7). Immunofluoresence of HA-IRS in the MCF-10A stable transfectants showed that approximately 5% of HA–IRS-1 and HA–IRS-2 was present in the nucleus; however, this level was unchanged following IGF treatment (data not shown). Despite this lack of IRS movement, MCF-10A cells overexpressing IRS-1 or IRS-2 showed elevated levels of the β-catenin target cyclin D1 gene levels, even though levels of cyclin A and B genes were unaltered (Fig. 8D).

DISCUSSION

In this study, we show for the first time that both human IRS-1 and IRS-2 are oncogenic when overexpressed in vivo. We also found that IRS-1 overexpression led to disruption of MCF-10A acinus morphogenesis. Transgenic mice overexpressing human IRS-1 or IRS-2 in the mammary gland showed progressive mammary hyperplasia, tumorigenesis, and metastasis. Mammary tumors from these mice showed mixed histologies with evidence for expansion of putative mammary progenitor cells. Consistent with this, IRSs were found to interact with β-catenin, an important regulator of stem/progenitor cell fate, and levels of β-catenin target c-*myc* and cyclin D1 genes were increased in both IRS-1 and IRS-2 mammary tumors. This is the first study to show that IRSs are oncogenes in vivo, and it highlights the growing literature that IRSs are critical signaling adaptor proteins in tumorigenesis.

The ability of IRSs to cause mammary tumorigenesis is intriguing, given that IRSs are signaling adaptors that have no intrinsic kinase activity and require upstream signals for activation and function. Indeed, mammary-specific overexpression of the signaling adaptor Grb2 failed to cause mammary tumors, and Shc overexpression resulted in very rare (7%) mammary tumors (54). In addition, overexpression of CrkL using its own promoter caused rare tumors in aged mice only and also didn't support a role for these adaptors as oncogenes in vivo (18), despite evidence that these genes can transform cell lines in vitro (46). Our study therefore highlights the importance of confirming transformation assays using in vivo model systems. One explanation for the oncogenic action of the IRSs maybe that they are able to signal to unique pathways compared to Grb2, Shc, and CrkL or that the IRSs are normally active in the mammary gland and, thus, when overexpressed, can sensitize

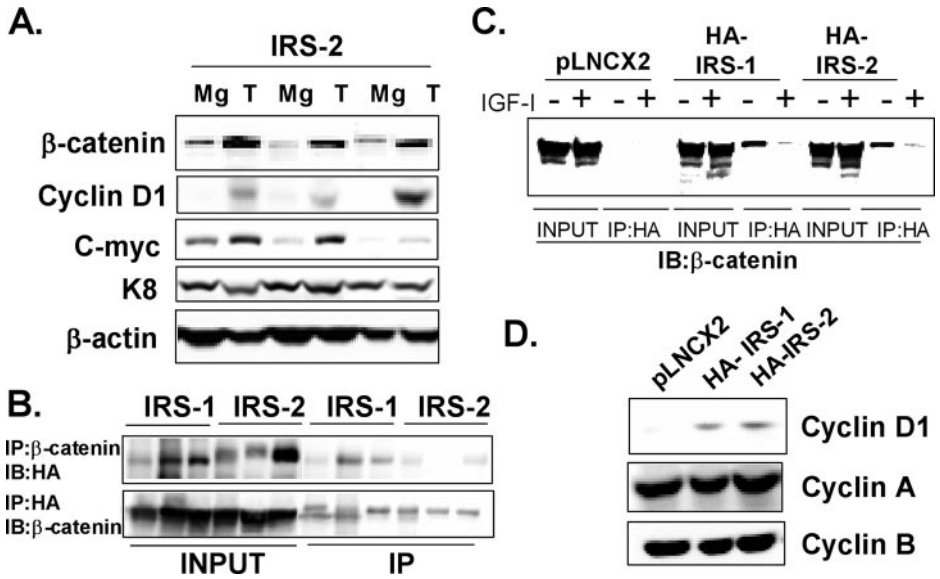

FIG. 8. MMTV-HA-IRS tumors show increased β-catenin levels and downstream signaling. (A) Representative immunoblotting of IRS-2 tumors (T) and mammary glands from the same transgenic mouse that did not contain a palpable or visible tumor upon dissection (Mg). Membranes were blotted for β-catenin, cyclin D1, and c-*myc* proteins. Keratin 8 served as a loading control for epithelial content, and β-actin served as a protein loading control. (B) Immunoprecipitation of HA or β-catenin followed by reciprocal HA or β-catenin immunoblotting from three HA-IRS-1 tumor lysates or three HA–IRS-2 tumor lysates. Input represents 75 μg of lysates, and 750 μg was used for the IP. (C) Immunoprecipitation of HA followed by β-catenin immunoblotting from MCF-10A cells stimulated with or without IGF-I (5 nM) for 24 h. Input represents 75 μg of lysates and 750 μg was used for the IP. (D) Immunoblotting of cell lysates from MCF-10A–HA–IRS-1 and MCF-10A–HA–IRS-2 clones for cyclin D1, A, or B.

these same pathways. Consistent with this is our observation that IRS tumors showed elevated Akt and ERK1/2 phosphorylation, and this was also noted to occur in MCF-10A–HA–IRS-1 and MCF-10A–HA–IRS-2 clones. Supporting this observation, transgenic overexpression of IRS-1 in the liver resulted in constitutive activation of phosphatidylinositol 3-kinase and ERK1/2, which resulted in enhanced DNA synthesis and greater liver mass (55).

The fact that IRS-1 is constitutively phosphorylated in the transgenic mice is important, given the similar observation for a number of different cancers (6), and that high levels of IRS-1 confer a poor prognosis in breast cancer (25). The reason for the constitutive phosphorylation of IRSs is currently unclear. It is possible that the IRSs are actually rate limiting in concentration and that overexpression sensitizes cells to upstream signals that are already active in the cell. This hypothesis is consistent with studies showing that IRS-1 overexpression (49) and loss (37) have dramatic effects in MCF-7 cells, whereas overexpression of its upstream activator, IGF-IR, has very minor effects. An alternative model for constitutive activation of IRSs is that they may cause reverse activation of their upstream signaling intermediates by causing receptor dimerization or oligomerization.

Overexpression of IRS-1 and overexpression of IRS-2 either in vitro or in vivo gave relatively similar phenotypes, despite previous evidence that the IRSs show overlapping but unique and nonredundant functions. For instance, studies with IRS-2 indicate a major role in cell motility (20) and invasion (47) which has been confirmed in vivo with genetic deletion of IRS-2, but not IRS-1, impeding metastasis of PyMT-induced mammary tumors (35). Surprisingly, in our studies, we found that overexpression of IRS-1 and overexpression of IRS-2 gave similar phenotypes in vitro and in vivo, and thus far, we have been unable to identify unique actions attributable to either. Indeed, the only difference we noted was that IRS-1 sensitized MCF-10A cells to IGF-I-stimulated ERK1/2 activation, whereas IRS-2 failed to cause a similar sensitization. Despite this, both IRS-1 and IRS-2 enhanced MCF-10A proliferation and disrupted morphogenesis, suggesting that both of these events are independent of ERK1/2. We did note that MMTV–HA–IRS-2 transgenic mice did show a shorter MTTF; however, comparison of the two different transgenic lines is hazardous, given potential differences in transgene integration sites, cell-specific expression levels, and transgene levels. In particular, an expression of IRSs in cells that didn't initially contain endogenous IRSs may have disrupted normal cell physiology. Importantly, however, we found that both IRS-1 and IRS-2 tumors were able to metastasize. It should be noted, however, that there were only three IRS-1 mammary tumors from which we could analyze metastasis. Further, more-detailed studies are under way to determine if there is a difference between IRS-1 and IRS-2 metastatic capacities; however, it is clear that IRS-1 mammary tumors can metastasize.

The time to form mammary tumors in IRS-1 and IRS-2 transgenic mice is relatively long, and this suggests a multistep process involving other cooperating oncogenes. Mouse mammary tumors pathology can be used to classify tumors according to the oncogenic pathways that have been activated (5). Thus, oncogenes from growth signaling pathways produce solid undifferentiated adenocarcinomas, whereas oncogenes that activate the canonical wnt/β-catenin signaling pathway produce well-differentiated tumors that contain both luminal and myo-

epithelial cells and often exhibit squamous transdifferentiation (33, 42). It has been hypothesized that this difference in tumor pathology is due to the ability of the growth factor pathways to transform cells that are committed to luminal epithelial differentiation, whereas wnt signaling may transform early progenitor cells that contain bipotent differentiation capability (Fig. 6F) (29). Consistent with this, wnt-1-derived tumors show expansion of putative progenitor cells that are not seen in ErbB2-driven tumors (30). In characterizing MMTV–HA–IRS-1 and MMTV–HA–IRS-2 tumors, we found that both sets of tumors showed similar pathologies which resembled those of wnt-activated tumors and not those of ErbB2-driven tumors. Consistent with this, we found multiple cell lineages and an expansion of both K6- and SCA-1-positive cells. Interestingly, during these studies, we also reported on the development of mammary tumors in transgenic mice that overexpress an activated IGF-IR in the mammary gland (4). These mice also developed tumors that showed both luminal and myoepithelial cells (K14 positive), squamous transdifferentiation, and expansion of K6-positive cells, thus phenocopying the IRS tumors. Mammary tumors arising from overexpression of des(1-3)-IGF-I in the mammary gland also revealed a propensity for high differentiation (papillary tumors), squamous transdifferentiation, and keratinization (17), and tumors arising from IGF-II overexpression also showed squamous components (39). Together, these data show that hyperactivation of IGF signaling via overexpression of ligands (IGF-I and IGF-II), receptors (IGF-IR), or downstream signaling intermediates (IRS-1 and IRS-2) causes highly differentiated tumors characterized by frequent squamous differentiation.

We found that, consistent with a mammary tumor phenotype indicating activation of the β-catenin signaling pathway in mammary transformation, IRSs could directly bind β-catenin, and IRS tumors showed an increased number of β-catenin target c-*myc* and cyclin D1 genes, a hallmark of tumors overexpressing a dominant active β-catenin (32a). Recent in vitro studies have shown that IGF-IR and IRSs may regulate the wnt/β-catenin signaling pathway. For instance, IGF-I has been shown to phosphorylate, stabilize, or cause nuclear translocation of β-catenin in colon (38), melanoma (43), and prostate cancer cells (52). In some systems, this regulation of β-catenin is associated with Tcf/Lef activity (12) and increased levels of β-catenin target genes (34). The regulation of β-catenin may in part be due to the fact that IGF-IR, IRS-1, E-cadherin, and β-catenin exist in a membrane complex in many cell types, and this complex is disrupted by IGF-I (16, 34), releasing stabilized β-catenin to signal in the nucleus. A similar finding has been seen with ErbB receptors, which synergistically interact with β-catenin (45). We also found that IRS-1 and IRS-2 coprecipitate with β-catenin and that this association was disrupted following IGF-I stimulation. Interestingly, it has recently been shown that IGF-I-mediated phosphorylation of ERK1/2 leads to binding to GSK3β, which is subsequently phosphorylated and deactivated, allowing release and stabilization of β-catenin (13). Given that we have shown both ERK1/2 and Akt activation downstream of IRSs, it is plausible that the cooperative activity of these pathways may stabilize and activate β-catenin in concert with the ability of IGF-I to disrupt an E-cadherin/IGF-IR/IRS/β-catenin complex and thus allow free stabilized β-catenin to signal.

Our work suggests an interaction between the IGF-IR/IRS signaling pathway and wnt/β-catenin in transformation. Recent studies have also implicated a similar interaction. For instance, loss of PTEN has been shown to increase wnt-1-mediated tumorigenesis (28). Furthermore, mammary specific overexpression of PTEN can partially inhibit wnt-1-induced mammary tumors, and this inhibition is via a reduction of IGF-IR levels and Akt activity (57).

IRS-1, in addition to being observed to interact with β-catenin, has recently been shown to directly bind, interact, and cooperate with numerous oncogene proteins, including JCV T antigen (21), simian virus 40 T antigen (14), ret oncoprotein (19, 32), and the ETV6-NTRK3 translocation oncoprotein (24). Importantly, downregulation of IRS-1 or elimination of its tyrosine phosphorylation can impair transformation by many of these oncogene proteins (8, 9, 14, 21). IRS-1 has also recently been shown to interact with several DNA binding proteins, including RAD51 (50), and have a nuclear function to regulate homologous recombinant DNA repair (HRR). Intriguingly, JCV T antigen can inhibit HRR via the recruitment of IRS-1 to RAD51. This inhibition of HRR is not seen in IRS-1-null cells and can be mimicked by IRS-1 containing an artificial nuclear localization sequence (40). It is therefore possible that IRS may cause tumorigenesis via interaction with multiple collaborating oncogenes.

In summary, we show here that IRS-1 and IRS-2 are oncogene proteins in the mammary gland in vivo and that tumorigenesis induced by these oncogene proteins indicates a role for progenitor cell expansion and β-catenin signaling. This study further supports the concept that IRSs are critical elements in tumorigenesis and provides novel models for the development of antagonists of IRS action.

ACKNOWLEDGMENTS

Human IRS-1 (pCMV-His-IRS-1) was a kind gift from Eiichi Araki, Kumamoto University, Japan, and human IRS-2 was from Lothar Vassen, University of Essen, Germany. Sophia Tsai provided the MMTV plasmid, and Senthil Muthuswamy provided the MCF-10A cells. The TROMA-I development by investigators Philippe Brulet and Rolf Kemler was obtained from the Developmental Studies Hybridoma Bank developed under the auspices of the NICHD and maintained by The University of Iowa, Department of Biological Sciences, Iowa City, IA. We thank ZaWaunyka Lazard for technical help with sectioning and IHC, Jessy George for helping with the initial generation of the transgenic mice, and Mike Lewis for advice and support with the confocal microscopy studies. We thank Yi Li, Jeff Rosen, Dan Medina, and Steffi Oesterreich (Baylor College of Medicine) for providing comments and advice on the manuscript. This work was supported in part by Public Health Service grants R01CA94118 (A.V.L.), P01CA30195 (A.V.L.), and R01DK52197 (D.L.H.).

Adrian V. Lee is the recipient of a T. T. Chao Scholar award from the Department of Medicine at Baylor College of Medicine. Robert K. Dearth was supported in part by a Training Program grant in Molecular Endocrinology (DK07696) and a Training Program grant in Translational Breast Cancer Research (CA90221).

REFERENCES

1. **Bergmann, U., H. Funatomi, M. Kornmann, H. G. Beger, and M. Korc.** 1996. Increased expression of insulin receptor substrate-1 in human pancreatic cancer. Biochem. Biophys. Res. Commun. **220:**886–890.
2. **Berlanga, J. J., O. Gualillo, H. Buteau, M. Applanat, P. A. Kelly, and M. Edery.** 1997. Prolactin activates tyrosyl phosphorylation of insulin receptor substrate 1 and phosphatidylinositol-3-OH kinase. J. Biol. Chem. **272:**2050–2052.
3. **Boissan, M., E. Beurel, D. Wendum, C. Rey, Y. Lecluse, C. Housset, M. L. Lacombe, and C. Desbois-Mouthon.** 2005. Overexpression of insulin recep-

tor substrate-2 in human and murine hepatocellular carcinoma. Am. J. Pathol. **167:**869–877.

4. **Carboni, J. M., A. V. Lee, D. L. Hadsell, B. R. Rowley, F. Y. Lee, D. K. Bol, A. E. Camuso, M. Gottardis, A. F. Greer, C. P. Ho, W. Hurlburt, A. Li, M. Saulnier, U. Velaparthi, C. Wang, M. L. Wen, R. A. Westhouse, M. Wittman, K. Zimmermann, B. A. Rupnow, and T. W. Wong.** 2005. Tumor development by transgenic expression of a constitutively active insulin-like growth factor I receptor. Cancer Res. **65:**3781–3787.
5. **Cardiff, R. D., E. Sinn, W. Muller, and P. Leder.** 1991. Transgenic oncogene mice. Tumor phenotype predicts genotype. Am. J. Pathol. **139:**495–501.
6. **Chang, Q., Y. Li, M. F. White, J. A. Fletcher, and S. Xiao.** 2002. Constitutive activation of insulin receptor substrate 1 is a frequent event in human tumors: therapeutic implications. Cancer Res. **62:**6035–6038.
7. **Chen, J., A. Wu, H. Sun, R. Drakas, C. Garofalo, S. Cascio, E. Surmacz, and R. Baserga.** 2005. Functional significance of type 1 insulin-like growth factor-mediated nuclear translocation of the insulin receptor substrate-1 and beta-catenin. J. Biol. Chem. **280:**29912–29920.
8. **D'Ambrosio, C., S. R. Keller, A. Morrione, G. E. Lienhard, R. Baserga, and E. Surmacz.** 1995. Transforming potential of the insulin receptor substrate 1. Cell Growth Differ. **6:**557–562.
9. **Deangelis, T., J. Chen, A. Wu, M. Prisco, and R. Baserga.** 2006. Transformation by the simian virus 40 T antigen is regulated by IGF-I receptor and IRS-1 signaling. Oncogene **25:**32–42.
10. **Debnath, J., and J. S. Brugge.** 2005. Modelling glandular epithelial cancers in three-dimensional cultures. Nat. Rev. Cancer **5:**675–688.
11. **Debnath, J., S. K. Muthuswamy, and J. S. Brugge.** 2003. Morphogenesis and oncogenesis of MCF-10A mammary epithelial acini grown in three-dimensional basement membrane cultures. Methods **30:**256–268.
12. **Desbois-Mouthon, C., A. Cadoret, M. J. Blivet-Van Eggelpoel, F. Bertrand, G. Cherqui, C. Perret, and J. Capeau.** 2001. Insulin and IGF-1 stimulate the beta-catenin pathway through two signalling cascades involving GSK-3beta inhibition and Ras activation. Oncogene **20:**252–259.
13. **Ding, Q., W. Xia, J. C. Liu, J. Y. Yang, D. F. Lee, J. Xia, G. Bartholomeusz, Y. Li, Y. Pan, Z. Li, R. C. Bargou, J. Qin, C. C. Lai, F. J. Tsai, C. H. Tsai, and M. C. Hung.** 2005. Erk associates with and primes GSK-3beta for its inactivation resulting in upregulation of beta-catenin. Mol. Cell **19:**159–170.
14. **Fei, Z. L., C. D'Ambrosio, S. Li, E. Surmacz, and R. Baserga.** 1995. Association of insulin receptor substrate 1 with simian virus 40 large T antigen. Mol. Cell. Biol. **15:**4232–4239.
15. **Green, J. E., and T. Hudson.** 2005. The promise of genetically engineered mice for cancer prevention studies. Nat. Rev. Cancer **5:**184–198.
16. **Guvakova, M. A., and E. Surmacz.** 1997. Overexpressed IGF-I receptors reduce estrogen growth requirements, enhance survival, and promote E-cadherin-mediated cell-cell adhesion in human breast cancer cells. Exp. Cell Res. **231:**149–162.
17. **Hadsell, D. L., K. L. Murphy, S. G. Bonnette, N. Reece, R. Laucirica, and J. M. Rosen.** 2000. Cooperative interaction between mutant p53 and des(1–3)IGF-I accelerates mammary tumorigenesis. Oncogene **19:**889–898.
18. **Hemmeryckx, B., A. van Wijk, A. Reichert, V. Kaartinen, R. de Jong, P. K. Pattengale, I. Gonzalez-Gomez, J. Groffen, and N. Heisterkamp.** 2001. Crkl enhances leukemogenesis in BCR/ABL P190 transgenic mice. Cancer Res. **61:**1398–1405.
19. **Hennige, A. M., R. Lammers, D. Arlt, W. Hoppner, V. Strack, G. Niederfellner, F. J. Seif, H. U. Haring, and M. Kellerer.** 2000. Ret oncogene signal transduction via a IRS-2/PI 3-kinase/PKB and a SHC/Grb-2 dependent pathway: possible implication for transforming activity in NIH3T3 cells. Mol. Cell. Endocrinol. **167:**69–76.
20. **Jackson, J. G., X. Zhang, T. Yoneda, and D. Yee.** 2001. Regulation of breast cancer cell motility by insulin receptor substrate-2 (IRS-2) in metastatic variants of human breast cancer cell lines. Oncogene **20:**7318–7325.
21. **Khalili, K., L. Del Valle, J. Y. Wang, N. Darbinian, A. Lassak, M. Safak, and K. Reiss.** 2003. T-antigen of human polyomavirus JC cooperates withIGF-IR signaling system in cerebellar tumors of the childhood-medulloblastomas. Anticancer Res. **23:**2035–2041.
22. **Koda, M., M. Sulkowska, L. Kanczuga-Koda, and S. Sulkowski.** 2005. Expression of insulin receptor substrate 1 in primary breast cancer and lymph node metastases. J. Clin. Pathol. **58:**645–649.
23. **Kosanke, S., S. M. Edgerton, D. Moore II, X. Yang, T. Mason, K. Alvarez, L. Jones, A. Kim, and A. D. Thor.** 2004. Mammary tumor heterogeneity in wt-ErbB-2 transgenic mice. Comp. Med. **54:**280–287.
24. **Lannon, C. L., M. J. Martin, C. E. Tognon, W. Jin, S. J. Kim, and P. H. Sorensen.** 2004. A highly conserved NTRK3 C-terminal sequence in the ETV6-NTRK3 oncoprotein binds the phosphotyrosine binding domain of insulin receptor substrate-1: an essential interaction for transformation. J. Biol. Chem. **279:**6225–6234.
25. **Lee, A. V., J. G. Jackson, J. L. Gooch, S. G. Hilsenbeck, E. Coronado-Heinsohn, C. K. Osborne, and D. Yee.** 1999. Enhancement of insulin-like growth factor signaling in human breast cancer: estrogen regulation of insulin receptor substrate-1 expression in vitro and in vivo. Mol. Endocrinol. **13:**787–796.
26. **Lee, A. V., P. Zhang, M. Ivanova, S. Bonnette, S. Oesterreich, J. M. Rosen, S. Grimm, R. C. Hovey, B. K. Vonderhaar, C. R. Kahn, D. Torres, J. George, S. Mohsin, D. C. Allred, and D. L. Hadsell.** 2003. Developmental and hormonal signals dramatically alter the localization and abundance of insulin receptor substrate proteins in the mammary gland. Endocrinology **144:**2683–2694.
27. **Lee, Y. H., and M. F. White.** 2004. Insulin receptor substrate proteins and diabetes. Arch. Pharm. Res. **27:**361–370.
28. **Li, Y., K. Podsypanina, X. Liu, A. Crane, L. K. Tan, R. Parsons, and H. E. Varmus.** 2001. Deficiency of Pten accelerates mammary oncogenesis in MMTV-Wnt-1 transgenic mice. BMC Mol. Biol. **2:**2.
29. **Li, Y., B. Welm, K. Podsypanina, S. Huang, M. Chamorro, X. Zhang, T. Rowlands, M. Egeblad, P. Cowin, Z. Werb, L. K. Tan, J. M. Rosen, and H. E. Varmus.** 2003. Evidence that transgenes encoding components of the Wnt signaling pathway preferentially induce mammary cancers from progenitor cells. Proc. Natl. Acad. Sci. USA **100:**15853–15858.
30. **Liu, B. Y., S. P. McDermott, S. S. Khwaja, and C. M. Alexander.** 2004. The transforming activity of Wnt effectors correlates with their ability to induce the accumulation of mammary progenitor cells. Proc. Natl. Acad. Sci. USA **101:**4158–4163.
31. **Ma, Z. Q., S. S. Chua, F. J. DeMayo, and S. Y. Tsai.** 1999. Induction of mammary gland hyperplasia in transgenic mice over-expressing human Cdc25B. Oncogene **18:**4564–4576.
32. **Melillo, R. M., F. Carlomagno, G. De Vita, P. Formisano, G. Vecchio, A. Fusco, M. Billaud, and M. Santoro.** 2001. The insulin receptor substrate (IRS)-1 recruits phosphatidylinositol 3-kinase to Ret: evidence for a competition between Shc and IRS-1 for the binding to Ret. Oncogene **20:**209–218.

32a. **Michaelson, J. S., and P. Leder.** 2001. β-Catenin is a downstream effector of Wnt-mediated tumorigenesis in the mammary gland. Oncogene **20:**5093–5099.

33. **Miyoshi, K., A. Rosner, M. Nozawa, C. Byrd, F. Morgan, E. Landesman-Bollag, X. Xu, D. C. Seldin, E. V. Schmidt, M. M. Taketo, G. W. Robinson, R. D. Cardiff, and L. Hennighausen.** 2002. Activation of different Wnt/beta-catenin signaling components in mammary epithelium induces transdifferentiation and the formation of pilar tumors. Oncogene **21:**5548–5556.
34. **Morali, O. G., V. Delmas, R. Moore, C. Jeanney, J. P. Thiery, and L. Larue.** 2001. IGF-II induces rapid beta-catenin relocation to the nucleus during epithelium to mesenchyme transition. Oncogene **20:**4942–4950.
35. **Nagle, J. A., Z. Ma, M. A. Byrne, M. F. White, and L. M. Shaw.** 2004. Involvement of insulin receptor substrate 2 in mammary tumor metastasis. Mol. Cell. Biol. **24:**9726–9735.
36. **Nehrbass, D., F. Klimek, and P. Bannasch.** 1998. Overexpression of insulin receptor substrate-1 emerges early in hepatocarcinogenesis and elicits preneoplastic hepatic glycogenosis. Am. J. Pathol. **152:**341–345.
37. **Nolan, M. K., L. Jankowska, M. Prisco, S. Xu, M. A. Guvakova, and E. Surmacz.** 1997. Differential roles of IRS-1 and SHC signaling pathways in breast cancer cells. Int. J. Cancer **72:**828–834.
38. **Playford, M. P., D. Bicknell, W. F. Bodmer, and V. M. Macaulay.** 2000. Insulin-like growth factor 1 regulates the location, stability, and transcriptional activity of beta-catenin. Proc. Natl. Acad. Sci. USA **97:**12103–12108.
39. **Pravtcheva, D. D., and T. L. Wise.** 1998. Metastasizing mammary carcinomas in H19 enhancers-Igf2 transgenic mice. J. Exp. Zool. **281:**43–57.
40. **Reiss, K., K. Khalili, A. Giordano, and J. Trojanek.** 2006. JC virus large T-antigen and IGF-I signaling system merge to affect DNA repair and genomic integrity. J. Cell. Physiol. **206:**295–300.
41. **Rocha, R. L., S. G. Hilsenbeck, J. G. Jackson, C. L. VanDenBerg, C. Weng, A. V. Lee, and D. Yee.** 1997. Insulin-like growth factor binding protein-3 and insulin receptor substrate-1 in breast cancer: correlation with clinical parameters and disease-free survival. Clin. Cancer Res. **3:**103–109.
42. **Rosner, A., K. Miyoshi, E. Landesman-Bollag, X. Xu, D. C. Seldin, A. R. Moser, C. L. MacLeod, G. Shyamala, A. E. Gillgrass, and R. D. Cardiff.** 2002. Pathway pathology: histological differences between ErbB/Ras and Wnt pathway transgenic mammary tumors. Am. J. Pathol. **161:**1087–1097.
43. **Satyamoorthy, K., G. Li, B. Vaidya, D. Patel, and M. Herlyn.** 2001. Insulin-like growth factor-1 induces survival and growth of biologically early melanoma cells through both the mitogen-activated protein kinase and beta-catenin pathways. Cancer Res. **61:**7318–7324.
44. **Schnarr, B., K. Strunz, J. Ohsam, A. Benner, J. Wacker, and D. Mayer.** 2000. Down-regulation of insulin-like growth factor-I receptor and insulin receptor substrate-1 expression in advanced human breast cancer. Int. J. Cancer **89:**506–513.
45. **Schroeder, J. A., M. C. Adriance, E. J. McConnell, M. C. Thompson, B. Pockaj, and S. J. Gendler.** 2002. ErbB-beta-catenin complexes are associated with human infiltrating ductal breast and murine mammary tumor virus (MMTV)-Wnt-1 and MMTV-c-Neu transgenic carcinomas. J. Biol. Chem. **277:**22692–22698.
46. **Senechal, K., J. Halpern, and C. L. Sawyers.** 1996. The CRKL adaptor protein transforms fibroblasts and functions in transformation by the BCR-ABL oncogene. J. Biol. Chem. **271:**23255–23261.
47. **Shaw, L. M.** 2001. Identification of insulin receptor substrate 1 (IRS-1) and IRS-2 as signaling intermediates in the α6β4 integrin-dependent activation of phosphoinositide 3-OH kinase and promotion of invasion. Mol. Cell. Biol. **21:**5082–5093.

48. **Sun, X. J., P. Rothenberg, C. R. Kahn, J. M. Backer, E. Araki, P. A. Wilden, D. A. Cahill, B. J. Goldstein, and M. F. White.** 1991. Structure of the insulin receptor substrate IRS-1 defines a unique signal transduction protein. Nature **352:**73–77.
49. **Surmacz, E., and J.-L. Burgard.** 1995. Overexpression of IRS-1 in the human breast cancer cell line MCF-7 induces loss of estrogen requirements for growth and transformation. Clin. Cancer Res. **1:**1429–1436.
50. **Trojanek, J., S. Croul, T. Ho, J. Y. Wang, A. Darbinyan, M. Nowicki, L. D. Valle, T. Skorski, K. Khalili, and K. Reiss.** 2006. T-antigen of the human polyomavirus JC attenuates faithful DNA repair by forcing nuclear interaction between IRS-1 and Rad51. J. Cell. Physiol. **206:**35–46.
51. **Vassen, L., W. Wegrzyn, and L. Klein-Hitpass.** 1999. Human insulin receptor substrate-2: gene organization and promoter characterization. Diabetes **48:**1877–1880.
52. **Verras, M., and Z. Sun.** 2005. Beta-catenin is involved in insulin-like growth factor 1-mediated transactivation of the androgen receptor. Mol. Endocrinol. **19:**391–398.
53. **Wakefield, L. M., G. Thordarson, A. I. Nieto, G. Shyamala, J. J. Galvez, M. R. Anver, and R. D. Cardiff.** 2003. Spontaneous pituitary abnormalities and mammary hyperplasia in FVB/NCr mice: implications for mouse modeling. Comp. Med. **53:**424–432.
54. **Webster, M. A., J. N. Hutchinson, M. J. Rauh, S. K. Muthuswamy, M. Anton, C. G. Tortorice, R. D. Cardiff, F. L. Graham, J. A. Hassell, and W. J. Muller.** 1998. Requirement for both Shc and phosphatidylinositol 3′ kinase signaling pathways in polyomavirus middle T-mediated mammary tumorigenesis. Mol. Cell. Biol. **18:**2344–2359.
55. **Wiedmann, M., S. Tamaki, R. Silberman, S. M. de la Monte, L. Cousens, and J. R. Wands.** 2003. Constitutive over-expression of the insulin receptor substrate-1 causes functional up-regulation of Fas receptor. J. Hepatol. **38:** 803–810.
56. **Yamauchi, T., Y. Kaburagi, K. Ueki, Y. Tsuji, G. R. Stark, I. M. Kerr, T. Tsushima, Y. Akanuma, I. Komuro, K. Tobe, Y. Yazaki, and T. Kadowaki.** 1998. Growth hormone and prolactin stimulate tyrosine phosphorylation of insulin receptor substrate-1, -2, and -3, their association with p85 phosphatidylinositol 3-kinase (PI3-kinase), and concomitantly PI3-kinase activation via JAK2 kinase. J. Biol. Chem. **273:**15719–15726.
57. **Zhao, H., Y. Cui, J. Dupont, H. Sun, L. Hennighausen, and S. Yakar.** 2005. Overexpression of the tumor suppressor gene phosphatase and tensin homologue partially inhibits wnt-1-induced mammary tumorigenesis. Cancer Res. **65:**6864–6873.